



PERGAMON

International Journal of Solids and Structures 38 (2001) 7381–7407

INTERNATIONAL JOURNAL OF
SOLIDS and
STRUCTURES

www.elsevier.com/locate/ijsolstr

On the macroscopic properties of discrete media with nearly periodic microstructures

M.W. Schraad *

Theoretical Division, Los Alamos National Laboratory, Group T-3, Mail Stop B216, Los Alamos, NM 87545, USA

Received 18 October 2000; in revised form 1 March 2001

Abstract

With recent improvements in fabrication processes, many structural components and solid materials are being designed at microstructural scales to provide specific macroscopic response characteristics. Optimal macroscopic properties and decreased susceptibilities to failure may be achieved by designing media with strictly periodic microstructures. Averaging and homogenization techniques, used to estimate the macroscopic properties of structured media, also are formulated on the basis of assumed microstructural periodicity. Few structures or materials, however, possess perfectly periodic microstructures. In the present work, the influence of perturbations in microstructural periodicity on the macroscopic response of structured media is investigated and quantified by examining the behavior of discrete media with both periodic and nearly periodic microstructures. The idealized macroscopic response of media with perfectly periodic microstructures is compared to the response obtained after perturbations in geometry and material properties are introduced into the models at the microstructural scale. Analysis shows that, for specific, well-defined classes of discrete media, the macroscopic properties are influenced only to second order in the perturbation amplitude parameter. In certain circumstances, however, the effects of these perturbations can become substantially more pronounced – demonstrating the limits of applicability of analysis techniques that assume that an underlying periodic microstructure exists for the discrete media under consideration. © 2001 Elsevier Science Ltd. All rights reserved.

Keywords: Macroscopic properties; Periodic microstructure; Perturbations

1. Introduction

Many structural components and essentially all solid materials possess some degree of relevant underlying microscopic structure. Large components such as multi-bay trusses and frames and materials such as honeycombs and structural composites are just a few examples of media with tailored microstructures that are used widely in engineering applications. Naturally, for these types of structures and materials, the mechanical response at the microstructural scale influences the corresponding macroscopic behavior. Often, small defects or irregularities in the microstructures will significantly and detrimentally affect not only the

* Fax: +1-505-665-5926.

E-mail address: schraad@lanl.gov (M.W. Schraad).

macroscopic response of these media, but ultimately the onset of failure as well. With recent improvements in fabrication processes, however, many structural components and solid materials now are being designed at microstructural scales to provide improved, or even desired, macroscopic response characteristics. For example, in the interest of producing structural components with optimal macroscopic properties and decreased susceptibilities to failure, cellular materials, such as metallic and ceramic honeycombs, often are designed to possess strictly periodic microstructures.

Few, if any, of the structural components and solid materials that are used in actual engineering applications possess perfectly periodic microstructures. And despite the additional simplicity that even assumed microstructural periodicity may offer to analysts, obtaining a fully resolved description of the mechanical response at the microstructural scale for these types of structures and materials is not, in general, analytically tractable or computationally feasible. Consequently, averaging and homogenization techniques are used extensively to estimate the macroscopic properties and obtain continuum-scale descriptions of the mechanical response for both continuous and discrete, structured media. These analytical techniques, which are formulated on the basis of assumed microstructural periodicity, most often are employed in applications involving media with nearly periodic microstructures, but often, in applications involving structures and solids with highly irregular or even random microstructures as well.

The development of analytical techniques for estimating the macroscopic properties of structured media has taken varied paths over the past several decades, and the literature is replete with examples of the various approximation methods that have been developed. In general, these analytical techniques fall into one of two broad categories. The first category includes methods for estimating the macroscopic properties of solid materials with random distributions of microscopic heterogeneities. For these techniques, the general concept of a representative volume element (RVE) that was introduced by Hill (1963) and Hashin (1964) is used to relate the macroscopic properties associated with an infinitesimal material neighborhood to the parameters that characterize the geometry and the properties of the constituents that compose the material neighborhood. Periodic boundary conditions are applied to the RVE, and the RVE must be statistically representative of the surrounding material. Using this approach, general averaging theorems have been developed for estimating the macroscopic properties of heterogeneous materials comprised of constituents that admit stress or strain potentials. Estimates of the macroscopic moduli and compliances of linear-elastic composite materials, using uniform strains and uniform stresses, are due to Voigt (1889, 1928) and Reuss (1929), respectively. These works center attention on the behavior of polycrystals, but the applications are much more broad. The fact that the Voigt and Reuss estimates actually provide bounds on the macroscopic properties has subsequently been shown by Hill (1952). Special averaging procedures, referred to as self-consistent methods, have been developed since by Hill (1965) and Budiansky (1965) for predicting the macroscopic properties of composite materials. Similarly, upper and lower bounding techniques for the macroscopic elastic moduli of structured media have been developed by Hashin and Shtrikman (1962a,b). The Hashin–Shtrikman variational principle has been generalized further by Willis (1977), and the general bounding procedure has been revisited and extended to include nonlinear constitutive behavior (see, e.g., Talbot and Willis, 1985, 1997; Castañeda, 1996; Castañeda and Willis, 1995).

The second category of analytical techniques includes methods for estimating the macroscopic properties of structural components with periodic microstructures and solid materials with periodic arrays of microscopic heterogeneities. As opposed to the concept of the statistically representative RVE, here the smallest representative microsection of the specimen, referred to as the unit cell, is used to approximate the macroscopic properties. For these techniques, it is assumed that the structural component or solid material comprises an infinite, spatially periodic collection of such unit cells. The macroscopic strain and stress fields in these media can be related to the parameters that characterize the geometry and the properties of each of the individual constituents, and in this manner, the macroscopic elastic moduli and compliances can be defined. An idealized elastic solid with periodic distributions of heterogeneities is “homogenized” by introducing appropriate periodically distributed eigenstrains or eigenstresses. Using this approach, the pe-

riodic elastic moduli are replaced by reference constant elastic moduli and an appropriate periodic eigenstrain field. The uniform solid with constant elastic moduli is referred to as the *equivalent homogeneous solid*. A detailed account of the formulation in terms of a Fourier series approach is given in Nemat-Nasser and Hori (1993). Asymptotic techniques applied to homogenization methods are provided by Sanchez-Palencia (1974) and Bensoussan et al. (1978).

In many structural components and composite materials the underlying microstructures can be well approximated as periodic. The aforementioned averaging and homogenization techniques, therefore, can be directly applied to such media – providing approximate values for the macroscopic properties. In addition, estimates of the macroscopic properties of structured media formed on the basis of *assumed* microstructural periodicity can provide limiting values for cases in which actual periodicity may be an idealization. Consequently, for applications involving media with highly irregular, and even random microstructures, these traditional averaging and homogenization techniques often are employed.

These two categories of approximation techniques represent media with microstructures at opposite ends of the possible spectrum, that is, those with statistically random microstructures and those with perfectly periodic microstructures, respectively. And while many solid materials with statistically random microstructures do exist, manufacturing tolerances, material impurities, defects, and damage preclude the fabrication of structural components and solid materials with perfectly periodic microstructures. From a design-engineering standpoint, an important issue exists regarding the quantification of the difference between the macroscopic properties predicted by techniques that assume microstructural periodicity and the actual properties of the *nearly* periodic solid or structure. Additionally, to the best of the author's knowledge, very little attention, if any, has been devoted to the development of approximation techniques that can be applied specifically to media with microstructures that lie somewhere between the extremes of statistical randomness and strict periodicity. A fundamental aspect of micromechanics, therefore, should focus on the issues concerning the influence of perturbations (or imperfections) in microstructural periodicity on the macroscopic response of structured media.

These issues, which appear to be neglected in traditional micromechanics analyses, are presently investigated by exploring the macroscopic response of discrete media (e.g., trusses, frames, cellular materials, etc.) with both periodic and nearly periodic microstructures. A nonisotropic, nonlinear-elastic truss structure and an initially isotropic, elasto-plastic honeycomb material are chosen as two particular models for study. The macroscopic response for each of these structured media is obtained first for the case when the underlying microstructures are modeled as perfectly periodic. This idealized behavior is then compared to the response obtained for the same models after perturbations in periodicity are introduced at the microstructural scale through imperfections in geometry and material properties. The shapes of the perturbations are arbitrary and the magnitudes are characterized by perturbation amplitude parameters. The results of detailed analysis, the main points of which are highlighted by several numerical examples involving the two models, show that, for specific, well-defined classes of discrete media, macroscopic quantities such as the strain energy density, from which the macroscopic stresses and the macroscopic incremental moduli are derived, are influenced only to second order in the perturbation amplitude parameter. In other equally well-defined circumstances, however, the effects of these perturbations can become substantially more pronounced – demonstrating the limits of applicability of analysis techniques that ideally assume that an underlying periodic microstructure exists for the discrete media under consideration.

2. Media with perfectly periodic microstructures

Before the macroscopic response of structural components and solid materials with nearly periodic microstructures can be examined, the macroscopic properties of media with perfectly periodic microstructures should be defined. General expressions for the macroscopic properties of media with periodic

microstructures are necessary for quantifying the influence of perturbations in microstructural periodicity on the corresponding idealized macroscopic behavior. In this section, general descriptions are provided for a class of discrete, structured media that are relevant to this investigation. Suitable micromechanical models are used to represent this class of discrete structures and materials, and these models are employed in the determination of the macroscopic response of the corresponding perfect specimens. The concepts of strain, stress, and strain energy are defined at the microstructural scale, and all underlying modeling assumptions are outlined. Mathematical expressions for the idealized macroscopic properties also are provided. These expressions are used later in the analysis to provide a standard by which comparison of the macroscopic properties for media with nearly periodic microstructures can be made.

2.1. Model descriptions

There are many types of engineering structures and materials that ideally possess discrete, periodic microstructures. Consider, for example, the structured media shown in Fig. 1a. Here, a two-dimensional truss (the joints and members of which do not support bending moments) and a two-dimensional frame (the joints and members of which do support bending moments) serve as examples of spatially periodic structures, whereas two cellular honeycombs with different microstructural geometries serve as examples of spatially periodic materials. Ideally, each of these specimens is a repetitive assembly of the corresponding smallest representative microsection or unit cell, as shown in Fig. 1b. The size of each unit cell is characterized by a microstructural length scale, h , which in three dimensions, is typically set equal to the cube root of the unit cell volume. Similarly, the size of the overall structure or material specimen is characterized by a macroscopic length scale, H , which is typically set equal to the cube root of the overall structural or specimen volume. A geometric scale parameter, ε , may be defined then as the ratio of these characteristic length scales (i.e., $\varepsilon = h/H$). As shown in previous studies (see Schraad and Triantafyllidis, 1997a,b; Triantafyllidis and Schraad, 1998), and as will be illustrated in the present investigation, the macroscopic response and the onset of failure in structured media may be strongly affected by this geometric scale parameter.

The macroscopic stress-strain response for media with periodic microstructures may be obtained by examining the behavior of suitably representative micromechanical models. For the class of discrete structures and materials presently under consideration, each representative microsection or unit cell is idealized as a collection of one-dimensional structural elements (e.g., springs, rods, beams, etc.). For purposes of illustration, the micromechanical models shown in Fig. 1a are all two dimensional. The forthcoming analysis, however, is applicable to discrete media with general, three-dimensional microstructures. Since the idealized models are spatially periodic, a given structural element of a particular unit cell necessarily possesses the identical geometry and material properties, and therefore, under homogeneous deformations, behaves identically to all of the corresponding elements in each of the remaining unit cells throughout the entire specimen. Naturally, as a result, the strains and stresses at the local material point scale within each structural element are spatially periodic as well under these conditions.

For the moment, consider each structural element within a particular unit cell to be a general, three-dimensional, solid body. Whenever changes take place in the relative positions of the parts of a solid body, that body is said to be strained. Many different strain measures exist for describing the continuous change of configuration of a solid body from one state to another (e.g., Green's, Almansi's, and Cauchy's strain tensors). Despite the differences among the various strain measures, they are all functions of the local material displacement field, which in turn, is a function of position within the given solid body. The particular choice of strain measure is immaterial to the present investigation, and so, let the components of the strain tensor at a given material point within the solid body be denoted by ϵ_{ij} , where

$$\epsilon_{ij} \equiv \epsilon_{ij}(\mathbf{u}(\theta, \phi, \psi)). \quad (1)$$

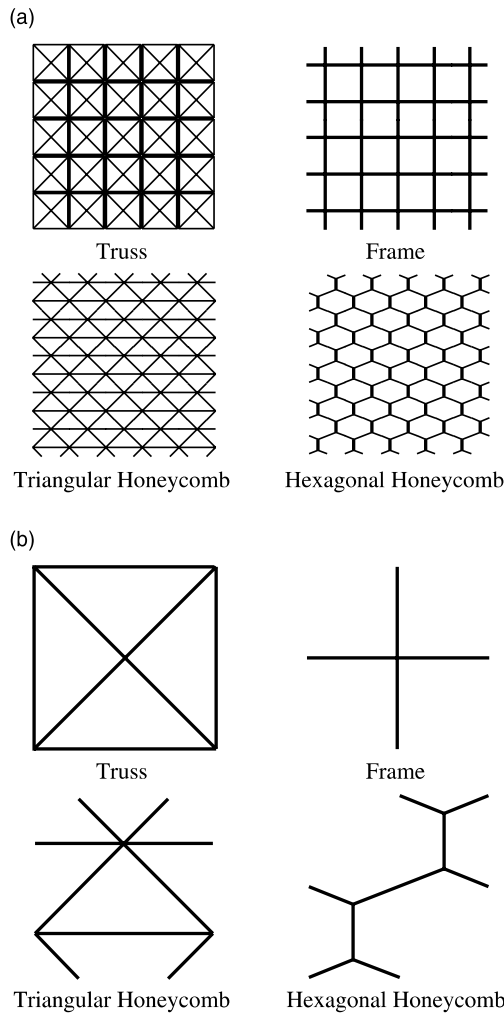


Fig. 1. Examples of: (a) spatially periodic structures and materials; and (b) the corresponding smallest representative microsections or unit cells.

Here, the vector $\mathbf{u}(\theta, \phi, \psi)$ is the displacement field at the material point in question, and θ , ϕ , and ψ represent the components of the initial position vector (i.e., the position in the reference or undeformed configuration) of the given material point in some convenient curvilinear coordinate system.

It is assumed that strain energy density functions, W , exist for the solid materials under consideration, and recall that, by definition, strain energy density functions exist for hyperelastic materials (see Noll, 1955). In the present analysis, thermal considerations are neglected, and therefore, the strain energy density function is assumed to be an analytic function of the strain tensor components alone. One physical case for which such a strain energy density function exists is when the changes that take place in a solid body are reversible and isothermal. Another physical case is when these changes are reversible and isentropic. These two possibilities cover many important practical applications within the fields of solid and structural mechanics. Under adiabatic conditions, W may be interpreted as the internal energy per unit mass, whereas under isothermal conditions, W may be identified with the free energy per unit mass. The corresponding

strain energy density functions under these two conditions are, in general, different functions. In either of these situations, however, the temperature does not appear explicitly in the functional form of W . A strain energy density function may exist in other thermal conditions. In these situations, however, it becomes necessary to exhibit the temperature dependence in the form of the strain energy density function. For a more detailed discussion on the existence of strain energy density functions, see Fung (1965) and Green and Zerna (1968).

With the existence of a strain energy density function under isothermal or adiabatic conditions, attention necessarily is restricted to materials that exhibit elastic (i.e., reversible) behavior – for at least some finite range of deformation in the neighborhood of the stress-free state. By definition, the state of stress in an elastic body is a unique function of the state of strain. It is possible then to choose the components of the strain tensor as the independent state variables and to express the strain energy density function as an analytic function of the strain tensor components alone (of course, W is also a function of the material properties – as will be shown directly). The stress tensor components, σ_{ij} , then are derivable from the strain energy density function:

$$\sigma_{ij} = \frac{\partial W}{\partial \epsilon_{ij}}. \quad (2)$$

Consider now a general constitutive law for nonlinear-elastic materials under isothermal or isentropic conditions. The corresponding strain energy density function can be expanded asymptotically (i.e., in a Taylor series) about the stress-free state to obtain

$$W = A + B_{ij}\epsilon_{ij} + \frac{1}{2}C_{ijkl}\epsilon_{ij}\epsilon_{kl} + \frac{1}{6}D_{ijklmn}\epsilon_{ij}\epsilon_{kl}\epsilon_{mn} + \dots, \quad (3)$$

where $A = W(\epsilon_{ij} = 0)$, $B_{ij} = dW(\epsilon_{ij} = 0)/d\epsilon_{ij}$, $C_{ijkl} = d^2W(\epsilon_{ij} = 0)/d\epsilon_{ij}d\epsilon_{kl}$, $D_{ijklmn} = d^3W(\epsilon_{ij} = 0)/d\epsilon_{ij}d\epsilon_{kl}d\epsilon_{mn}$, etc. are the constant properties that characterize the stress–strain response of the material in question. Consequently, the components of the stress tensor take on the following form:

$$\sigma_{ij} = B_{ij} + C_{ijkl}\epsilon_{kl} + \frac{1}{2}D_{ijklmn}\epsilon_{ij}\epsilon_{kl}\epsilon_{mn} + \dots \quad (4)$$

Without loss of generality, the strain energy density function may be defined to be identically equal to zero when all of the strain tensor components are equal to zero. As a result, $A \equiv 0$. Furthermore, under isothermal or isentropic conditions, the stress tensor components must all be identically equal to zero when all of the strain components are equal to zero. As a result, $B_{ij} \equiv 0$, and therefore, the strain energy density function and the stress–strain relation take on the following forms, respectively:

$$W = \frac{1}{2}C_{ijkl}\epsilon_{ij}\epsilon_{kl} + \frac{1}{6}D_{ijklmn}\epsilon_{ij}\epsilon_{kl}\epsilon_{mn} + \dots \quad (5)$$

and

$$\sigma_{ij} = C_{ijkl}\epsilon_{kl} + \frac{1}{2}D_{ijklmn}\epsilon_{kl}\epsilon_{mn} + \dots, \quad (6)$$

where C_{ijkl} are now recognized as the familiar linear-elastic moduli and D_{ijklmn} , etc. are higher-order elastic moduli that characterize the nonlinearity in the material response.

It is important to note at this point that the forthcoming analysis is based on the existence of a strain energy density function for the materials under consideration. And, as previously mentioned, this assumption necessarily restricts attention to materials that exhibit elastic behavior for at least some range of deformation. This does not mean, however, that the analysis is restricted to materials that only behave elastically. When a material is strained beyond the elastic limit, the constitutive relations outlined in Eqs. (5) and (6) may be augmented, for example, with a yield condition and a plastic flow rule to obtain an elasto-plastic constitutive law. Other inelastic constitutive laws also may be considered, and various models that account for the accumulation of continuum material damage (e.g., porosity) may be included in the ma-

terial response description. Once the material behavior leaves the elastic range, however, the response is no longer reversible, and hence, a strain energy density function no longer exists. The forthcoming analysis, therefore, applies to materials that have not been strained beyond their elastic limit and have not accumulated any amount of continuum material damage.

Now, recall that the micromechanical models currently under consideration comprise collections of one-dimensional structural elements (generalization of the forthcoming analysis to solid materials with continuum microstructures will appear in a sequel to this work). Each element within a given model is assumed to be a hyperelastic solid. Consider a given structural element of a particular unit cell of an arbitrary micromechanical model. Label this element e , and denote the corresponding strain, stress, strain energy, etc., with the superscript e . For general extensional and bending deformations of the structural element, the only nonnegligible stress component is the axial stress. Denote this stress component by σ^e and the corresponding axial strain component by ϵ^e . That is, the element strain and element stress are given, respectively, by

$$\epsilon^e \equiv \epsilon^e(\mathbf{u}^e(\theta, \phi, \psi)) \quad \text{and} \quad \sigma^e = C^e \epsilon^e + \frac{1}{2} D^e (\epsilon^e)^2 + \dots, \quad (7)$$

and therefore, the element strain energy density function is given by

$$W^e = \frac{1}{2} C^e (\epsilon^e)^2 + \frac{1}{6} D^e (\epsilon^e)^3 + \dots, \quad (8)$$

where \mathbf{u}^e is now the local displacement field of the element in question. Here, $C^e = C_{1111}$ is the lone linear-elastic material constant and $D^e = D_{111111}$, etc. are the higher-order elastic material constants, which characterize not only the nonlinearity in the response of the element in question, but the nonlinearity in the response of the entire micromechanical model as well.

The total strain energy stored in a given structural element, \mathcal{E}^e , is simply the integral of the strain energy density taken over the volume of the element. That is,

$$\mathcal{E}^e = \int_{V^e} W^e \, dV = \int_{V^e} \left[\frac{1}{2} C^e (\epsilon^e)^2 + \frac{1}{6} D^e (\epsilon^e)^3 + \dots \right] dV, \quad (9)$$

where V^e is the total volume of the structural element in question. Now, since only one-dimensional structural elements are being considered, let A^e and l^e denote the cross-sectional area and the length of the structural element, respectively. Then, the relation for the element strain energy becomes

$$\mathcal{E}^e = \int_{A^e} \int_0^{l^e} \left[\frac{1}{2} C^e (\epsilon^e)^2 + \frac{1}{6} D^e (\epsilon^e)^3 + \dots \right] ds \, dA, \quad (10)$$

where s denotes the arc-length parameter for the structural element. Here, without loss of generality, it is assumed that the cross-sectional area is constant along the length of the structural element and that the material properties are constant throughout the element volume. If this were not the case, then the cross-sectional area, A^e , would be a function of s and the material properties, C^e , D^e , etc. would be functions of s , y , and z . These assumptions maintain the discrete nature of the forthcoming analysis and do not affect the corresponding results.

Now, since the element strain is a function of the local element displacement field, the element strain energy assumes the following functional form:

$$\mathcal{E}^e \equiv \mathcal{E}^e(A^e, l^e(\mathbf{X}^e), C^e, D^e, \dots, \mathbf{u}^e), \quad (11)$$

where \mathbf{X}^e denotes the vector of element end positions (e.g., in three dimensions, the vector \mathbf{X}^e has six components – three components of the position vector for each end of the element). In other words, the element strain energy depends on the geometry of the element, the element material properties, and the deformed configuration of the element.

2.2. Macroscopic properties

Of primary interest is the development and appropriate use of macroscopic constitutive laws for structured media that are based upon mechanical response occurring at microstructural scales. Traditionally, continuum descriptions, obtained through macroscopic averaging and homogenization techniques, are used to model the macroscopic response of structured media. For the structures and materials with perfectly periodic microstructures presently under consideration, definitions for the macroscopic properties are based on a definition for the macroscopic strain energy density.

The macroscopic strain energy density, denoted by W , is defined to be the volume average of the total strain energy stored in the specimen, denoted by \mathcal{E} . This quantity, in turn, is simply equal to the sum of the element strain energies, \mathcal{E}^e , defined in Eq. (10). That is,

$$W = \frac{1}{V} \mathcal{E} = \frac{1}{V} \sum_{c=1}^{N_c} \left[\sum_{e=1}^{N_e} \mathcal{E}^e \right]_c = \frac{N_c}{H^3} \sum_{e=1}^{N_e} \mathcal{E}^e, \quad (12)$$

where N_c is the total number of unit cells in the entire micromechanical model and N_e is the number of structural elements per unit cell. The last equality in Eq. (12) holds, since for periodic specimens, every unit cell responds identically to a given homogeneous macroscopic deformation. Naturally, this implies that

$$\mathcal{E}^e = \text{constant} \quad \forall c \in \{1, \dots, N_c\}, \quad (13)$$

and consequently, the macroscopic response of periodic media can be determined from the behavior of the corresponding unit cells.

Several different macroscopic stress tensors, such as Lagrange's stress tensor and the first and second Piola–Kirchhoff stress tensors, can be derived from the macroscopic strain energy density. The forthcoming analysis is independent of the choice of stress measure, so as an example, consider the nonsymmetric, first Piola–Kirchhoff stress tensor, $\mathbf{\Pi}$, which is defined by

$$\mathbf{\Pi} = \frac{\partial W}{\partial \mathbf{F}} = \frac{N_c}{H^3} \sum_{e=1}^{N_e} \frac{\partial \mathcal{E}^e}{\partial \mathbf{F}}. \quad (14)$$

Here, \mathbf{F} is the macroscopic deformation gradient tensor, which for homogeneous deformations, may be determined from the prescribed displacements on the boundary of the specimen. Similarly, the macroscopic incremental moduli tensor, \mathbf{L} , which relates the increments in the stress tensor components, Π_{ij} , to the increments in the deformation gradient tensor components, F_{ij} , is defined by

$$\mathbf{L} = \frac{\partial^2 W}{\partial \mathbf{F} \partial \mathbf{F}} = \frac{N_c}{H^3} \sum_{e=1}^{N_e} \frac{\partial^2 \mathcal{E}^e}{\partial \mathbf{F} \partial \mathbf{F}}. \quad (15)$$

In the next section, the influence of perturbations in microstructural periodicity on the idealized macroscopic properties, W , $\mathbf{\Pi}$, and \mathbf{L} , is examined and quantification of this influence is pursued analytically. The idealized response obtained using these macroscopic property definitions is compared then to the behavior obtained numerically for two models with small perturbations in the periodicity of the underlying microstructures.

3. Media with nearly periodic microstructures

In the previous section, relations were developed for the macroscopic stress and the macroscopic incremental moduli tensors for a class of structured media with discrete, three-dimensional, periodic mi-

crostructures. The structures and materials under consideration are assumed to exhibit hyperelastic behavior (i.e., it is assumed that a strain energy density function exists) for at least some range of deformation in the neighborhood of the stress-free state. Also, since these media are discrete, it is also assumed that the microstructures can be modeled accurately as collections of one-dimensional structural elements. In this way, the macroscopic strain energy density, on which the definitions for the macroscopic properties are based, can be defined as a volume average of the sum of the individual element strain energies. Furthermore, the periodic nature of the underlying microstructures permits evaluation of the macroscopic response of each specimen by restricting attention to the behavior of a single unit cell.

Of course, few of the structural components and solid materials used in actual engineering applications possess perfectly periodic microstructures. Manufacturing tolerances and damage induced during fabrication processes inevitably result in, at least, small imperfections in the underlying microstructural geometries. Similarly, impurities and continuum damage in the parent materials necessarily lead to imperfections in the properties that govern the solid material response. As a result, structured media can possess, at best, nearly periodic microstructures. Consequently, the periodic micromechanical models are idealizations, and the macroscopic properties that are determined from analyses that are based on the assumption of strict periodicity can only provide approximations or limits to the macroscopic properties of the actual media with nearly periodic microstructures. To obtain a more realistic description of the macroscopic response for these types of structural components and solid materials, consideration must be given to the imperfections that exist in the underlying microstructures and to the corresponding influence of these imperfections on the macroscopic properties of the media in question.

3.1. Perturbations in microstructural periodicity

With the aforementioned issues regarding microstructural imperfections in mind, consider an arbitrary structural element of an arbitrary unit cell for any particular micromechanical model with an initially periodic microstructure. Next, consider the following geometric and material property perturbations, which naturally destroy the original periodicity of the model. The perturbed cross-sectional area for this structural element is given by

$$A^e = \mathring{A}^e(1 + \delta r_A^e), \quad \text{where } -1 \leq r_A^e \leq 1. \quad (16)$$

Similarly, the components of the perturbed element end position vector are given by

$$X_i^e = \mathring{X}_i^e + \delta h r_i^e = \mathring{X}_i^e + \delta e H r_i^e, \quad \text{where } -1 \leq r_i^e \leq 1 \text{ for } i = 1, 2, \dots, 6. \quad (17)$$

And finally, the perturbed material properties for this structural element are given by

$$C^e = \mathring{C}^e(1 + \delta r_C^e), \quad D^e = \mathring{D}^e(1 + \delta r_D^e), \text{ etc.}, \quad \text{where } -1 \leq r_C^e, r_D^e, \dots \leq 1. \quad (18)$$

Here, \mathring{A}^e , \mathring{X}_i^e , \mathring{C}^e , \mathring{D}^e , etc. are the cross-sectional area, the end positions, and the material properties of the element in the perfectly periodic configuration, respectively; δ is the perturbation amplitude parameter; and r_A^e , r_i^e , r_C^e , r_D^e , etc. are the parameters that characterize the shapes of the microstructural perturbations in geometry and material properties. In the previous section, it was assumed that the cross-sectional area of each structural element remained constant along the element length and that the material properties were uniform throughout the volume of each element. Without loss of generality, this assumption is retained here. If the element area, A^e , was allowed to vary along the length of the element and the material properties, C^e , D^e , etc., were allowed to vary spatially within each element, the forthcoming analysis would become slightly more complex, while the results of the analysis would remain unchanged. Since the

micromechanical models are constructed with collections of one-dimensional elements, this assumption maintains the discrete nature of the analysis.

The preceding geometric and material property perturbations naturally lead to a displacement field that also depends on the perturbation amplitude parameter. That is,

$$\mathbf{u} \equiv \mathbf{u}(\delta). \quad (19)$$

The dependence of the geometry, the material properties, and the displacements on the perturbation amplitude parameter dictates that the macroscopic properties of this particular micromechanical model depend on δ as well. The remainder of this section, therefore, is devoted to quantifying the effects of these microstructural perturbations on the macroscopic properties of structured media.

3.2. Influence on the macroscopic strain energy density

Since for hyperelastic materials the macroscopic stress tensor, $\mathbf{\Pi}$, and the macroscopic incremental moduli tensor, \mathbf{L} , can be defined in terms of the macroscopic strain energy density, W , it is possible to quantify the influence of perturbations in microstructural periodicity on these macroscopic properties by examining the corresponding effect on W . This is accomplished most easily by examining the different terms in an asymptotic expansion of the strain energy density, which is taken about the periodic solution (i.e., about the point $\delta = 0$). The expansion of the macroscopic strain energy density is given by

$$W(\delta, \mathbf{u}(\delta)) = W|_{\delta=0} + \delta \frac{dW}{d\delta} \Big|_{\delta=0} + \frac{\delta^2}{2} \frac{d^2W}{d\delta^2} \Big|_{\delta=0} + O(\delta^3), \quad (20)$$

where the total derivative in the first-order term of the expansion may be expressed as

$$\frac{dW}{d\delta} = \frac{\partial W}{\partial \delta} + \frac{\partial W}{\partial \mathbf{u}} \cdot \frac{d\mathbf{u}}{d\delta}, \quad (21)$$

and the total derivative in the second-order term may be expressed as

$$\frac{d^2W}{d\delta^2} = \frac{\partial^2 W}{\partial \delta^2} + \frac{\partial^2 W}{\partial \mathbf{u} \partial \delta} \cdot \frac{d\mathbf{u}}{d\delta} + \frac{\partial W}{\partial \mathbf{u}} \cdot \frac{d^2\mathbf{u}}{d\delta^2} + \left(\frac{\partial^2 W}{\partial \mathbf{u} \partial \delta} + \frac{d\mathbf{u}}{d\delta} \cdot \frac{\partial^2 W}{\partial \mathbf{u} \partial \mathbf{u}} \right) \cdot \frac{d\mathbf{u}}{d\delta}. \quad (22)$$

These relations may be simplified considerably by examining the equilibrium equations of the nearly periodic specimen. The most compact form of the equilibrium equations are given by

$$\frac{\partial \mathcal{E}}{\partial \mathbf{u}} \cdot \delta \mathbf{u} = 0 \text{ in } V; \quad \text{and} \quad \delta \mathbf{u} = 0 \text{ on } \partial V. \quad (23)$$

Here, V is the total volume of the specimen, ∂V denotes the specimen boundary, and $\delta \mathbf{u}$ is any kinematically admissible field. Recall that the perturbed element end positions are given by Eq. (17), and therefore, the displacement component, u_k^e , corresponding to the end position of an element, e , which lies on the boundary of the specimen, is prescribed by

$$u_k^e = (F_{ki} - I_{ki})X_i^e = (F_{ki} - I_{ki})(\dot{X}_i^e + \delta \varepsilon H r_i^e). \quad (24)$$

Consequently,

$$\frac{1}{H} \frac{d u_k^e}{d \delta} = \varepsilon (F_{ki} - I_{ki}) r_i^e \rightarrow 0 \quad \text{on } \partial V \text{ as } \varepsilon \rightarrow 0 \quad (25)$$

and

$$\frac{d^2 u_k^e}{d \delta^2} = 0 \quad \text{on } \partial V. \quad (26)$$

Since $du_k^e/d\delta$ and $d^2u_k^e/d\delta^2$ are kinematically admissible fields, equilibrium considerations dictate that the following relations hold:

$$\frac{1}{H} \frac{\partial \mathcal{E}}{\partial \mathbf{u}} \cdot \frac{d\mathbf{u}}{d\delta} \rightarrow 0 \text{ in } V; \quad \text{and} \quad \frac{1}{H} \frac{d\mathbf{u}}{d\delta} \rightarrow 0 \text{ on } \partial V \text{ as } \varepsilon \rightarrow 0 \quad (27)$$

and

$$\frac{\partial \mathcal{E}}{\partial \mathbf{u}} \cdot \frac{d^2\mathbf{u}}{d\delta^2} = 0 \text{ in } V; \quad \text{and} \quad \frac{d^2\mathbf{u}}{d\delta^2} = 0 \text{ on } \partial V. \quad (28)$$

As a result, for media with a characteristic microstructural length scale that is small relative to the overall structural dimensions (i.e., when $h \ll H \Rightarrow \varepsilon \rightarrow 0$), the following relations can be developed:

$$\frac{\partial W}{\partial \mathbf{u}} \cdot \frac{d\mathbf{u}}{d\delta} = \frac{1}{H^3} \frac{\partial \mathcal{E}}{\partial \mathbf{u}} \cdot \frac{\partial \mathbf{u}}{\partial \delta} = 0 \quad \text{and} \quad \frac{\partial W}{\partial \mathbf{u}} \cdot \frac{d^2\mathbf{u}}{d\delta^2} = \frac{1}{H^3} \frac{\partial \mathcal{E}}{\partial \mathbf{u}} \cdot \frac{d^2\mathbf{u}}{d\delta^2} = 0. \quad (29)$$

Furthermore, by taking the derivative of the equilibrium equations with respect to the perturbation amplitude parameter, the following relation can be obtained:

$$\left(\frac{\partial^2 \mathcal{E}}{\partial \mathbf{u} \partial \delta} + \frac{d\mathbf{u}}{d\delta} \cdot \frac{\partial^2 \mathcal{E}}{\partial \mathbf{u} \partial \mathbf{u}} \right) \cdot \delta \mathbf{u} = 0 \text{ in } V; \quad \text{and} \quad \delta \mathbf{u} = 0 \text{ on } \partial V. \quad (30)$$

Therefore, when $h \ll H$, the following additional relation also can be developed:

$$\left(\frac{\partial^2 W}{\partial \mathbf{u} \partial \delta} + \frac{d\mathbf{u}}{d\delta} \cdot \frac{\partial^2 W}{\partial \mathbf{u} \partial \mathbf{u}} \right) \cdot \frac{d\mathbf{u}}{d\delta} = 0, \quad (31)$$

which leads to

$$\frac{\partial^2 W}{\partial \mathbf{u} \partial \delta} \cdot \frac{d\mathbf{u}}{d\delta} = - \frac{d\mathbf{u}}{d\delta} \cdot \frac{\partial^2 W}{\partial \mathbf{u} \partial \mathbf{u}} \cdot \frac{d\mathbf{u}}{d\delta} < 0. \quad (32)$$

The inequality in Eq. (32) holds for deformations occurring prior to initial bifurcation in the principal equilibrium solution. In these situations, the potential energy stored in the specimen at equilibrium is a minimum and is stable, and therefore, the incremental stiffness matrix, $\partial^2 \mathcal{E} / \partial \mathbf{u} \partial \mathbf{u}$, must be positive definite (see, for example, Love (1944)).

Thus, for nearly periodic media with $h \ll H$, the derivatives in the first- and second-order terms in the expansions of the macroscopic strain energy densities simplify considerably. Using the relations developed in Eqs. (29), (31), and (32), the derivatives given in Eqs. (21) and (22) reduce, respectively, to

$$\frac{dW}{d\delta} = \frac{\partial W}{\partial \delta} \quad (33)$$

and

$$\frac{d^2 W}{d\delta^2} = \frac{\partial^2 W}{\partial \delta^2} + \frac{\partial^2 W}{\partial \mathbf{u} \partial \delta} \cdot \frac{d\mathbf{u}}{d\delta}, \quad \text{where} \quad \frac{\partial^2 W}{\partial \mathbf{u} \partial \delta} \cdot \frac{d\mathbf{u}}{d\delta} < 0. \quad (34)$$

Now, Eqs. (33) and (34) may be simplified further by considering the influence of perturbations in microstructural periodicity on the individual terms remaining in the expansions. Therefore, consider the first-order term, evaluated at the point $\delta = 0$. This term may be rewritten as

$$\frac{dW}{d\delta} \Big|_{\delta=0} = \frac{\partial W}{\partial \delta} \Big|_{\delta=0} = \frac{1}{H^3} \sum_{e=1}^{N_e} \sum_{c=1}^{N_c} \left[\frac{\partial \mathcal{E}^e}{\partial \delta} \Big|_{\delta=0} \right]_c. \quad (35)$$

Recalling Eq. (11), it can be seen that, for nearly periodic media, each element strain energy assumes the following functional form:

$$\mathcal{E}^e \equiv \mathcal{E}^e(\delta, \mathbf{u}(\delta)) \equiv \mathcal{E}^e(A^e(\delta), l^e(X_i^e(\delta)), C^e(\delta), D^e(\delta), \dots, u_k^e(\delta)). \quad (36)$$

Therefore, the partial derivative of the element strain energy with respect to the perturbation amplitude parameter is given, via the chain rule, by

$$\frac{\partial \mathcal{E}^e}{\partial \delta} = \frac{\partial \mathcal{E}^e}{\partial A^e} \frac{\partial A^e}{\partial \delta} + \frac{\partial \mathcal{E}^e}{\partial l^e} \frac{\partial l^e}{\partial X_i^e} \frac{\partial X_i^e}{\partial \delta} + \frac{\partial \mathcal{E}^e}{\partial C^e} \frac{\partial C^e}{\partial \delta} + \frac{\partial \mathcal{E}^e}{\partial D^e} \frac{\partial D^e}{\partial \delta} + \dots, \quad (37)$$

where summation is implied on the repeated index i .

The partial derivatives $\partial A^e / \partial \delta$, $\partial X_i^e / \partial \delta$, $\partial C^e / \partial \delta$, $\partial D^e / \partial \delta$, etc. can be found quite easily from the expressions given in Eqs. (16)–(18). Thus, evaluating the expression given in Eq. (37) at the point $\delta = 0$ provides the following relation:

$$\left[\frac{\partial \mathcal{E}^e}{\partial \delta} \right]_{\delta=0} = \left[\frac{\partial \mathcal{E}^e}{\partial A^e} \right]_{\delta=0} \dot{A}^e r_A^e + \left[\frac{\partial \mathcal{E}^e}{\partial l^e} \right]_{\delta=0} \frac{\partial l^e}{\partial X_i^e} \Big|_{\delta=0} h r_i^e + \left[\frac{\partial \mathcal{E}^e}{\partial C^e} \right]_{\delta=0} \dot{C}^e r_C^e + \left[\frac{\partial \mathcal{E}^e}{\partial D^e} \right]_{\delta=0} \dot{D}^e r_D^e + \dots \quad (38)$$

Terms in this relation that are evaluated at the point $\delta = 0$ correspond to those of the periodic specimen. Therefore, for any arbitrary element, e , the following relations must hold:

$$\left[\frac{\partial \mathcal{E}^e}{\partial A^e} \right]_{\delta=0} \Big|_c \equiv c_A = \text{constant} \quad \forall c \in \{1, \dots, N_c\}, \quad (39)$$

$$\left[\frac{\partial \mathcal{E}^e}{\partial l^e} \right]_{\delta=0} \Big|_c \equiv c_l = \text{constant} \quad \forall c \in \{1, \dots, N_c\}, \quad (40)$$

$$\left[\frac{\partial \mathcal{E}^e}{\partial X_i^e} \right]_{\delta=0} \Big|_c \equiv c_i = \text{constant} \quad \forall c \in \{1, \dots, N_c\}, \quad (41)$$

$$\left[\frac{\partial \mathcal{E}^e}{\partial C^e} \right]_{\delta=0} \Big|_c \equiv c_C = \text{constant} \quad \forall c \in \{1, \dots, N_c\}, \quad (42)$$

$$\left[\frac{\partial \mathcal{E}^e}{\partial D^e} \right]_{\delta=0} \Big|_c \equiv c_D = \text{constant} \quad \forall c \in \{1, \dots, N_c\}. \quad (43)$$

In other words, since each term on the left-hand sides of Eqs. (39)–(43) is evaluated at the point $\delta = 0$, any term evaluated for a given structural element of a particular unit cell has the identical value as the corresponding term evaluated for the corresponding element in each of the remaining unit cells throughout the entire specimen, and hence, is constant for all $c \in \{1, \dots, N_c\}$.

Furthermore, for certain classes of perturbation shapes, the following identities involving the parameters that characterize the shapes of the microstructural perturbations can be established:

$$\sum_{c=1}^{\infty} [r_A^e]_c = \sum_{c=1}^{\infty} [r_i^e]_c = \sum_{c=1}^{\infty} [r_C^e]_c = \sum_{c=1}^{\infty} [r_D^e]_c = \dots \equiv 0 \quad \forall e \in \{1, \dots, N_e\}. \quad (44)$$

These relations hold, for example, if $h \ll H$ and the parameters $r_A^e, r_i^e, r_C^e, r_D^e$, etc., are statistically random (see, for example, Mendenhall et al. (1990)), or if the parameters $r_A^e, r_i^e, r_C^e, r_D^e$, etc., are themselves periodic

in nature with a period equal to an integral fraction of the overall structural dimension, H . Many other examples of perturbations shapes can be given, for which the identities provided in Eq. (44) hold, and in general, many types of structural and material imperfections that arise from errors induced during manufacturing processes satisfy Eq. (44).

Since the terms in relations (39)–(43) are constant, the identities given in Eq. (44) can be used to obtain the following additional identities:

$$\sum_{c=1}^{N_c} \left[\frac{\partial \mathcal{E}^e}{\partial A^e} \Big|_{\delta=0} \dot{A}^e r_A^e \right]_c = c_A \dot{A}^e \sum_{c=1}^{N_c} [r_A^e]_c \equiv 0 \quad \forall e \in \{1, \dots, N_e\}, \quad (45)$$

$$\sum_{c=1}^{N_c} \left[\frac{\partial \mathcal{E}^e}{\partial l^e} \Big|_{\delta=0} \frac{\partial l^e}{\partial X_i^e} \Big|_{\delta=0} h r_i^e \right]_c = c_l c_i h \sum_{c=1}^{N_c} [r_i^e]_c \equiv 0 \quad \forall e \in \{1, \dots, N_e\}, \quad (46)$$

$$\sum_{c=1}^{N_c} \left[\frac{\partial \mathcal{E}^e}{\partial C^e} \Big|_{\delta=0} \dot{C}^e r_C^e \right]_c = c_C \dot{C}^e \sum_{c=1}^{N_c} [r_C^e]_c \equiv 0 \quad \forall e \in \{1, \dots, N_e\}, \quad (47)$$

$$\sum_{c=1}^{N_c} \left[\frac{\partial \mathcal{E}^e}{\partial D^e} \Big|_{\delta=0} \dot{D}^e r_D^e \right]_c = c_D \dot{D}^e \sum_{c=1}^{N_c} [r_D^e]_c \equiv 0 \quad \forall e \in \{1, \dots, N_e\}. \quad (48)$$

In other words, the identities provided in Eq. (44) can be used to demonstrate that each quantity on the left-hand sides of Eqs. (45)–(48) is identically equal to zero. Consequently, substitution of the identities provided by Eqs. (45)–(48) into Eq. (38) and substitution of the result into Eq. (35) provides the following identity for the first-order term in the expansion of the macroscopic strain energy density:

$$\frac{dW}{d\delta} \Big|_{\delta=0} = \frac{\partial W}{\partial \delta} \Big|_{\delta=0} \equiv 0. \quad (49)$$

In exactly the same manner, it can be shown that

$$\frac{\partial^2 W}{\partial \delta^2} \Big|_{\delta=0} = 0, \quad (50)$$

and therefore

$$\frac{d^2 W}{d\delta^2} \Big|_{\delta=0} = \frac{\partial^2 W}{\partial \mathbf{u} \partial \delta} \frac{d\mathbf{u}}{d\delta} \Big|_{\delta=0} < 0. \quad (51)$$

3.3. Influence on the macroscopic properties

The result of the preceding analysis is that Eq. (20) may be reduced to

$$W = W|_{\delta=0} + \frac{\delta^2}{2} \frac{d^2 W}{d\delta^2} \Big|_{\delta=0} + O(\delta^3) < W|_{\delta=0}, \quad (52)$$

which, through the definitions provided by Eqs. (14) and (15), naturally leads to the following relations:

$$\mathbf{\Pi} = \mathbf{\Pi}|_{\delta=0} + \frac{\delta^2}{2} \frac{d^2 \mathbf{\Pi}}{d\delta^2} \Big|_{\delta=0} + O(\delta^3) \quad (53)$$

and

$$\mathbf{L} = \mathbf{L}|_{\delta=0} + \frac{\delta^2}{2} \frac{d^2\mathbf{L}}{d\delta^2} \Big|_{\delta=0} + \mathcal{O}(\delta^3). \quad (54)$$

The main conclusions reached through this analysis are summarized best by Eqs. (49)–(51), or alternatively by Eqs. (52)–(54). These equations state quite simply that the first-order term in the expansion of the macroscopic strain energy density is identically equal to zero and that the corresponding second-order term is less than zero prior to initial bifurcation in the principal equilibrium solution. In other words, the influence of perturbations in microstructural periodicity on the macroscopic properties of initially periodic media are second order in the perturbation amplitude parameter and the energy-carrying capacities of these structures and materials are decreased by these microstructural perturbations. These results, of course, rely on the assumption that the solid materials under consideration are exhibiting hyperelastic behavior, and therefore, possess a strain energy density function. Additionally, necessary and sufficient conditions for relations (52)–(54) to hold are that the specimens under consideration possess a characteristic microstructural length scale that is small relative to the overall structural dimensions (i.e., that $h \ll H$ and thus $\epsilon \rightarrow 0$) and that the parameters that characterize the shape of the microstructural perturbations satisfy Eq. (44).

In the next section, the macroscopic mechanical response of discrete media with both periodic and nearly periodic microstructures is explored numerically. A nonlinear-elastic truss structure and an elasto-plastic honeycomb material are chosen as two particular models for study. The macroscopic response for each of these structured media is obtained first for the case when the underlying microstructures are assumed to be perfectly periodic. This idealized behavior is then compared to the response obtained for the same models after perturbations in periodicity are introduced at the microstructural scale through imperfections in geometry and material properties.

4. Numerical examples

In the previous section, consideration was given to several different classes of imperfections that may be present in the underlying microstructures of the structural components and the solid materials currently under investigation. It was shown that the difference between the macroscopic properties of structured media with nearly periodic microstructures and the macroscopic properties of the corresponding, perfectly periodic structures and materials are second order in the amplitude parameter that characterizes the magnitude of the imperfection. These results hold for specimens comprised of hyperelastic materials, provided that the microstructures are sufficiently refined, that the imperfection shapes satisfy certain criteria (see Section 3.2), and that the deformations remain in the hyperelastic regime of behavior. To more clearly illustrate how these types of microstructural imperfections influence the macroscopic response of various structured media, several numerical examples now are considered. Two particular micromechanical models – a nonisotropic structural model and an initially isotropic cellular material model – are used to demonstrate under which conditions the main analytical results of the previous section hold.

To quantify the influence of perturbations in microstructural periodicity on the macroscopic properties of media with initially periodic microstructures, two dimensionless parameters are defined. First, a dimensionless strain energy density parameter, C , is used to measure the normalized difference in the macroscopic strain energy density between models with nearly periodic microstructures and their corresponding periodic counterparts. This dimensionless parameter is defined by

$$C = \frac{|W - W_0|}{|W_0|}, \quad (55)$$

where W_0 is the macroscopic strain energy density of the periodic model (i.e., $W_0 = W(\delta = 0)$). Similarly, a dimensionless stress parameter, D , is used to measure the normalized difference in the first Piola–Kirchhoff stress tensor between the nearly periodic and the perfectly periodic models. This dimensionless parameter is defined by

$$D = \frac{\|\boldsymbol{\Pi} - \boldsymbol{\Pi}_0\|}{\|\boldsymbol{\Pi}_0\|}, \quad (56)$$

where $\boldsymbol{\Pi}_0$ is the first Piola–Kirchhoff stress tensor of the periodic model (i.e., $\boldsymbol{\Pi}_0 = \boldsymbol{\Pi}(\delta = 0)$).

It is also useful to define the limits of the two parameters, C and D , as the geometric scale parameter, ε , approaches zero. Denote these limits as C_0 and D_0 , respectively (i.e., $C_0 = \lim_{\varepsilon \rightarrow 0} C$ and $D_0 = \lim_{\varepsilon \rightarrow 0} D$). The two dimensionless parameters, C and D , and their corresponding limits, C_0 and D_0 , are used in this section to quantify the effects of perturbations in microstructural periodicity on the macroscopic properties of the elastic truss model and the aluminum honeycomb model. Since it has been shown analytically that the influence of these perturbations is second order in the perturbation amplitude parameter, δ , for media with sufficiently refined microstructures, it is expected that, for a given load path, both C and D will converge to nonzero, finite values as ε decreases. Furthermore, as dictated by the results of the previous analysis, it is expected that each of these values will be proportional to the square of δ for deformations that remain in the hyperelastic regime of behavior.

4.1. Nearly periodic structures – nonlinear-elastic truss models

First, consider the elastic truss model shown in Fig. 1a (upper left). This model is particularly suited for the present investigation, because it is relatively simple – involving only one-dimensional truss elements – yet it possesses the complexity necessary to exhibit the effects of microstructural perturbations on the resulting macroscopic properties. This micromechanical model has been used by the author in previous investigations, and therefore, a detailed discussion of the geometry, the material properties, the element constitutive behavior, and the prescribed boundary conditions is provided elsewhere (for a description of this model see Schraad and Triantafyllidis, 1997a). For reasons of completeness, however, a short presentation of the salient features of this model is provided below.

Consideration is given to finite deformations of the elastic truss model, and therefore, nonlinear kinematic relations are required for describing the element strains. Since all nonlinear strain measures are equivalent in one spatial dimension, for convenience, the Lagrangian strain is adopted. This element strain measure, denoted by ϵ^e , is given by

$$\epsilon^e = \frac{1}{2} \left[\left(\frac{l^e}{L^e} \right)^2 - 1 \right], \quad (57)$$

where L^e and l^e are the lengths of the structural element in the reference (i.e., the undeformed) and the current (i.e., the deformed) configurations, respectively. The element strain energy, \mathcal{E}^e is taken to be

$$\mathcal{E}^e = A^e E^e L^e \left[\frac{1}{2}(\epsilon^e)^2 + (\text{sgn } \epsilon^e) \frac{1}{3} a^e (\epsilon^e)^3 + \frac{1}{4} b^e (\epsilon^e)^4 \right], \quad (58)$$

where $A^e = \mathcal{A}^e \varepsilon$ is the cross-sectional area of the structural element, E^e is the initial tangent modulus of the element material, and the quantities a^e and b^e are element material constants. Note that the cross-sectional area of each structural element scales with the size of the unit cell to provide a macroscopic stress–strain response that is independent of the geometric scale parameter, ε – for models with perfectly periodic microstructures. The following values of the material properties are used in the present investigation: $\mathcal{A}^e = 1$, $E^e = 1$, $a^e = -7/2$, and $b^e = 7/2$. These constants are adopted for all subsequent calculations involving the

periodic model, because they give rise to a macroscopic stress–strain response with a broad nonlinear range and a maximum load at a finite level of strain.

The truss model is subjected to fully prescribed displacement boundary conditions corresponding to uniaxial tension without transverse contraction. This particular load path does not provide a unique demonstration of the model's behavior, but rather is chosen simply as a matter of convenience and for purposes of illustration. The displacement vector for each constrained boundary node is given by

$$\mathbf{u}|_{\mathbf{X} \in \partial V} = \{\Delta X_1 \ 0\}^T, \quad (59)$$

where $\mathbf{X} = \{X_1, X_2\}$ represents the nodal position vector, ∂V denotes the boundary of the specimen, and Δ is the macroscopic displacement parameter that characterizes the level of deformation to which the specimen is subjected. Thus, for the case of uniaxial tension without transverse contraction, the truss model is subjected to a state of biaxial stress with principal stresses that are both positive.

The principal stress–strain solution is obtained first for a model with periodic microstructure and then for various models with small perturbations in microstructural periodicity. Random perturbations in the element cross-sectional areas, the element tangent moduli, and the element nodal positions are all considered (see Section 3.1 for a more detailed discussion of how these microstructural perturbations are introduced into the models). The solutions for both the periodic model and the nearly periodic models are compared and the convergence of the dimensionless parameters, C and D , is examined, as the geometric scale parameter, ε , decreases. The dependence of the corresponding limits, C_0 and D_0 , on the perturbation amplitude parameter, δ , is also explored. Additional comparisons are made to provide a more thorough understanding of the manner in which these perturbations influence the macroscopic response of the model. And finally, the actual stress–strain behavior for both the periodic and the nearly periodic truss models is investigated and appropriate comparisons are made.

So first, consider the convergence of the dimensionless strain energy density parameter, C , and the dimensionless stress parameter, D , as the geometric scale parameter, ε , decreases (i.e., as the microstructure of the truss model becomes more refined). It is expected that C and D will vary most widely when the microstructure is relatively coarse (i.e., when ε is large) and will converge to a relatively constant value as the microstructure is refined. This outcome seems reasonable, since the first-order term in the expansion of the macroscopic strain energy density, W , approaches zero as the geometric scale parameter approaches zero. Indeed, Fig. 2a and b, respectively, shows that C and D converge to relatively constant values as ε approaches zero (i.e., as $1/\varepsilon$ increases).

In Fig. 2a, the dimensionless strain energy density parameter is determined for various nearly periodic truss models with values of the geometric scale parameter ranging from 0.333 ($N_c = 9$) to 0.0333 ($N_c = 900$). To better represent the distribution of behavior, 10 different microstructural perturbations are considered for each value of ε . Each perturbation corresponds to a different random shape. In addition, for each perturbation shape, three different values of the perturbation amplitude parameter, δ , are considered. Results are presented for levels of deformation corresponding to $\Delta = 0.05$.

The numerical values to which C converges as ε approaches zero are represented by solid, dotted, and dashed lines for values of δ corresponding to 0.08, 0.16, and 0.24, respectively. As expected, the results show that these constant values increase as δ increases. The variations in C that are present for large values of ε are due to variations in the first-order terms in the expansions of W . As the geometric scale parameter decreases, however, this first-order effect diminishes. Therefore, for suitably small values of ε , the variations in C become due solely to differences between the second-order terms in the expansions of W for the various perturbed microstructures that are considered for the elastic truss models under investigation. In other words, the variations are due to differences in microstructural geometry. The convergence of the dimensionless strain energy density parameter is quite rapid, however, and for values of ε smaller than approximately 0.1 ($1/\varepsilon \simeq 10$), the value of C remains relatively constant.

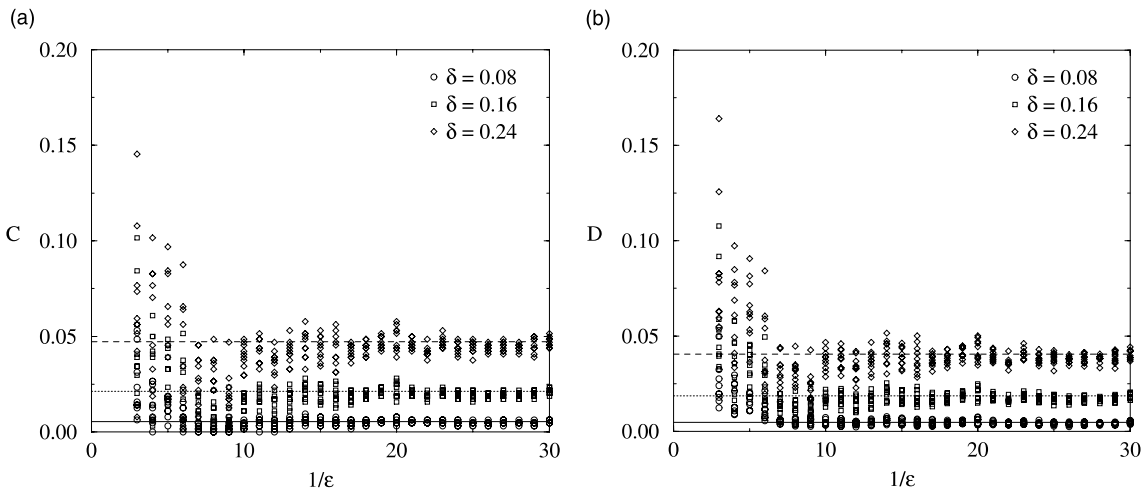


Fig. 2. Convergence of: (a) the dimensionless strain energy density parameter; and (b) the dimensionless stress parameter, as the microstructure of the elastic truss model is refined. The lines represent the limiting values of the two parameters as $\varepsilon \rightarrow 0$.

In Fig. 2b, the dimensionless stress parameter is determined for exactly the same values of the geometric scale parameter and perturbation amplitude parameter and for the same random perturbation shapes. Similar to the behavior of the dimensionless strain energy density parameter, D converges to relatively constant values as ε approaches zero. Again, the numerical values to which D converges as ε approaches zero are represented by solid, dotted, and dashed lines for values of δ corresponding to 0.08, 0.16, and 0.24, respectively. And, as expected, the results show that these constant values increase as δ increases (since the first Piola–Kirchhoff stress tensor, Π , is derived from the macroscopic strain energy density). Again, the variations in D for small values of ε are due solely to differences between the second-order terms in the expansions of Π (or W) for models with different perturbation shapes.

The influence of these perturbations in microstructural periodicity on the macroscopic properties of the truss model is characterized best by examining the dependence of the limits of the two dimensionless parameters on the perturbation amplitude parameter. In Fig. 3a and b, C_0 and D_0 are plotted as functions of the perturbation amplitude parameter for truss models with $\varepsilon = 0.04$ and for values of δ ranging from 0.00 to 0.25. For each value of δ , 10 different random perturbation shapes are considered. And again, results are presented for levels of deformation corresponding to $\Delta = 0.05$.

It becomes evident from these results that the limits of both the dimensionless strain energy density parameter and the dimensionless stress parameter are influenced by the perturbation amplitude parameter only to second order, as suggested by the quadratic dependence of C_0 and D_0 on δ . Recall that these results can be predicted directly from Eqs. (52) and (53) for specimens of sufficient microstructural refinement (i.e., sufficient to guarantee that Eq. (44) holds).

In addition to predicting the second-order influence of perturbations in periodicity on the macroscopic properties, Eq. (52) also predicts that these perturbations lead to a decrease in the macroscopic strain energy density for a given level of deformation. In Fig. 4a, the normalized value of W (i.e., the ratio of W for a truss model with microstructural perturbations to W for the corresponding periodic model) is plotted as a function of the perturbation amplitude parameter for truss models with $\varepsilon = 0.04$. Again, for each value of δ , 10 different random perturbation shapes are considered. The results clearly illustrate the detrimental effect of microstructural perturbations on the macroscopic strain energy density of these structures. The damaging influence of these perturbations becomes even more apparent when consideration is given to the effects on the macroscopic stress response of the structure.

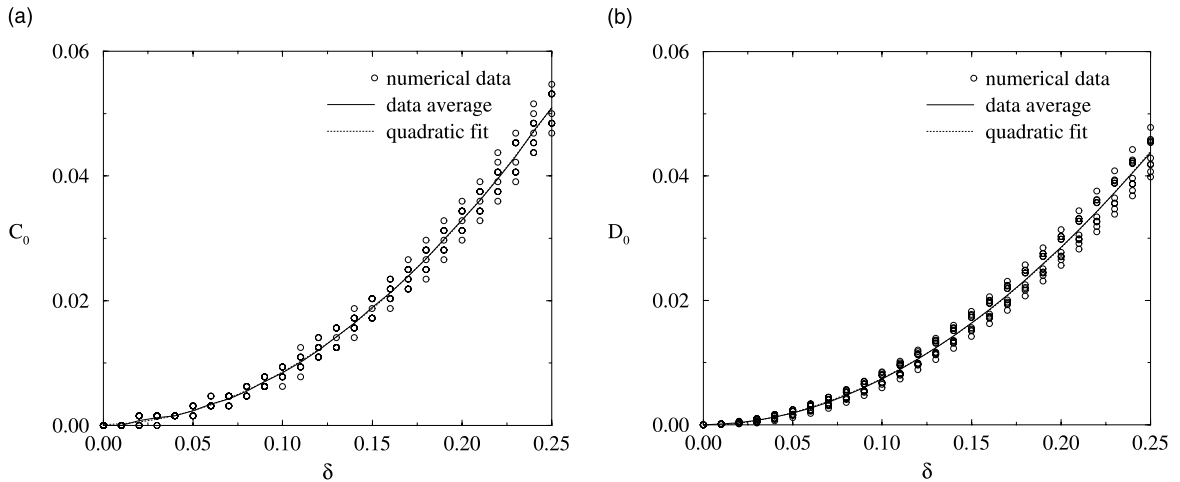


Fig. 3. Limiting values of: (a) the dimensionless strain energy density parameter; and (b) the dimensionless stress parameter, plotted as functions of the perturbation amplitude parameter. The data averages and the corresponding quadratic fit to these data are represented by the solid and dotted curves, respectively.

In Fig. 4b, the ratio of macroscopic stress tensor norms corresponding to the results presented in Fig. 4a is plotted as a function of the perturbation amplitude parameter. Again, the results show that any perturbation in periodicity has a detrimental effect on the macroscopic stress norm for a given level of deformation. These results simply indicate that a truss model with nearly periodic microstructure has a lower overall load-carrying capacity than the corresponding periodic model.

Despite the detrimental effect of perturbations in microstructural periodicity on the macroscopic stress tensor norm, the influence of these perturbations on the individual components of the stress tensor depends on the actual perturbation shape and the direction of macroscopic loading. In Fig. 5, the normalized stress tensor components (i.e., the ratios of Π_{ij} for a truss model with nearly periodic microstructure to Π_{ij} for the corresponding periodic model) are plotted versus the perturbation amplitude parameter for truss models with $\epsilon = 0.04$. The results presented here correspond directly to those presented in Fig. 4b. It is clearly evident from these results that the given microstructural perturbations cause a decrease in one component of the macroscopic stress tensor and an increase in the other (recall that the deformation under consideration is uniaxial, and therefore, leads to negligible values for the macroscopic shear stress components, Π_{12} and Π_{21}). Depending on the prescribed loading conditions and the shapes of the microstructural perturbations, the individual components of Π may be affected in many different ways. The influence on the macroscopic response, however, is always detrimental to the overall “performance” of the structure and second order in the perturbation amplitude parameter.

Finally, the most illuminating illustration of how perturbations in microstructural periodicity influence the macroscopic properties of the elastic truss structure may be provided by comparing the actual macroscopic stress response of a nearly periodic model with the behavior of the corresponding periodic model. In Fig. 6, the macroscopic stress tensor components (normalized with respect to the initial tangent modulus of the perfectly periodic material), are plotted as functions of Δ for truss models with both periodic and nearly periodic microstructures and with $\epsilon = 0.04$. For the nearly periodic model, a rather large perturbation amplitude parameter, $\delta = 0.24$, is prescribed to better demonstrate the resulting effects. The results illustrate that the effect of the microstructural perturbations on the macroscopic stress response is relatively small – even for the large value of δ that is prescribed. These small effects, however, are consistent with the

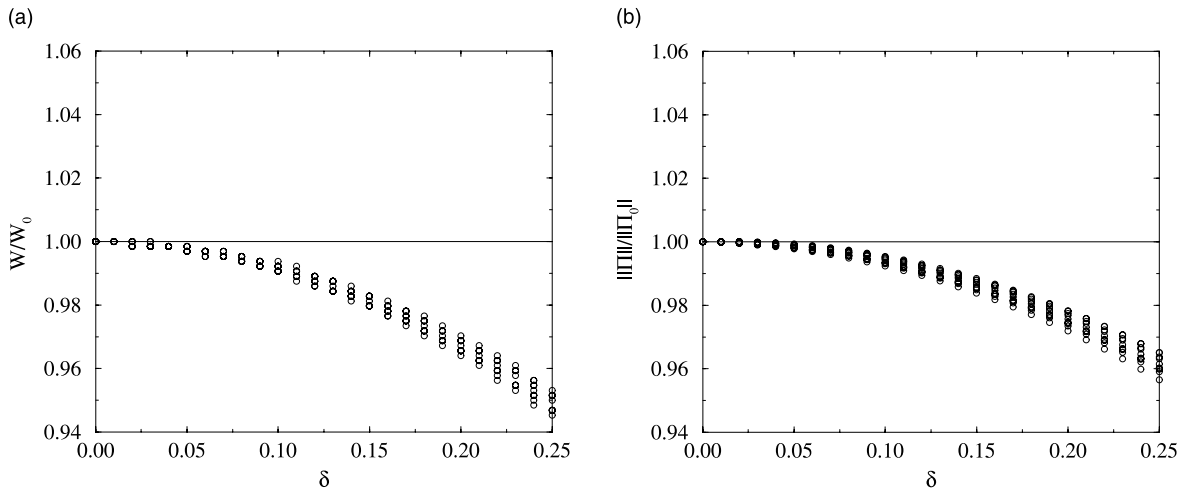


Fig. 4. Normalized values of: (a) the macroscopic strain energy density; and (b) the macroscopic stress tensor norm, plotted as functions of the perturbation amplitude parameter.

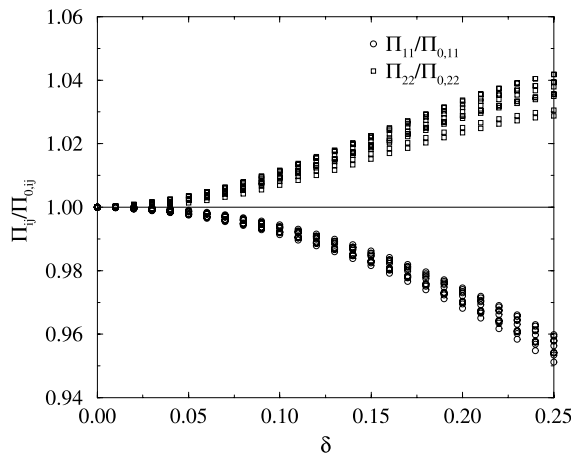


Fig. 5. Normalized values of the macroscopic stress tensor components plotted as functions of the perturbation amplitude parameter.

predicted second-order influence and may be misleading, as the stress level at failure may be affected significantly (see Schraad and Triantafyllidis, 1997b).

Note that the macroscopic stress response for the periodic model is plotted for a range of deformations corresponding to $0.0 \leq \Delta \leq 0.2$, however, the behavior for the nearly periodic model is plotted only for those deformations that occur prior to initial failure (here, initial failure is defined as the occurrence of the first bifurcation or buckling-type instability in the periodic model and the corresponding limit or maximum load in the nearly periodic model). Also note that, despite the relatively minor effect on the macroscopic stress for a given level of deformation, the stress at failure is significantly lower than the maximum stress attained by the periodic structure. Lastly, notice that one component of the macroscopic stress tensor experiences a decrease due to the perturbations in periodicity, but that the other component experiences an increase (these results correspond to those presented in Fig. 5). Keep in mind, however, that the total

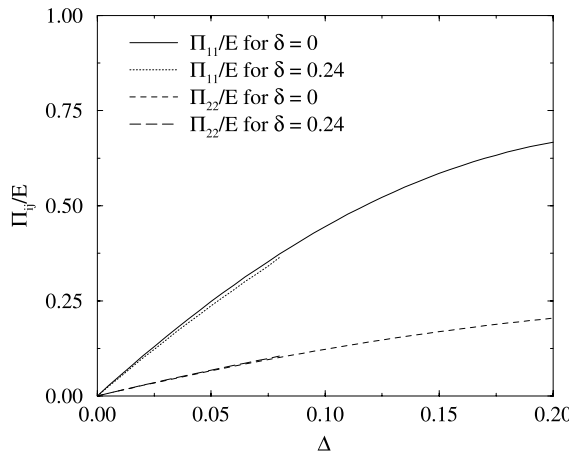


Fig. 6. Macroscopic stress response for elastic truss models with both periodic and nearly periodic microstructures subjected to uniaxial tension with no lateral contraction.

macroscopic strain energy density corresponding to a given level of deformation, by definition, experiences a decrease due to microstructural perturbations.

4.2. Nearly periodic cellular materials – aluminum honeycomb models

Next, consider a material with a slightly more complicated underlying microstructure – specifically, an aluminum honeycomb with a two-dimensional, hexagonal-lattice microstructure similar to that shown in Fig. 1a (lower right). Due to the elasto-plastic nature of the aluminum and the bending of the thin cell walls that results during in-plane compressive loadings of these materials, the mechanical response at the microstructural scale is much more complicated than the corresponding behavior exhibited by the elastic truss model that was previously analyzed. In the reference configuration, the microstructure of the aluminum honeycomb material consists of a regular hexagonal lattice. If the nominal hexagonal cell size is denoted by c , then the length of each cell wall is given by $c/\sqrt{3}$.

Typically, metallic honeycombs are manufactured by bonding strips of the parent material together at specific locations and then pulling the ensemble apart into the appropriate configuration. If the thickness of the aluminum strips used in this process is denoted by t , then the thickness of each of the vertical cell walls of the honeycomb material is given by $2t$, and the thickness of the remaining cell walls is given by t . Nevertheless, each of the cell walls is very thin, and when subjected to in-plane, compressive stress states, deforms essentially through bending. Hence, the cell walls are idealized as nonlinear beams that may undergo arbitrarily large displacements and rotations. The corresponding beam theory that is used to model this behavior is a generalization of the elastica beam theory that is due to Euler. The present theory, however, accounts for axial deformations as well. This theory has been proposed elsewhere (see, for example, Love, 1944; Antman, 1968), and therefore, is not presented here.

An elasto-plastic constitutive law is used to describe the relationship between the element axial stress component (i.e., the only nonnegligible stress component), σ^e , and the corresponding element axial strain component, ϵ^e . This constitutive behavior is modeled using a standard bilinear relationship given by

$$\sigma^e = \begin{cases} E\epsilon^e & \text{for } \epsilon^e \leq \epsilon_y, \\ E\epsilon_y + E_t(\epsilon^e - \epsilon_y) & \text{for } \epsilon^e > \epsilon_y, \end{cases} \quad (60)$$

where E represents the initial tangent modulus of the material, ϵ_y is the value of axial strain at the onset of plasticity, and E_t denotes the post-yield, tangent modulus of the material.

The following values of the material constants are used in the present investigation: $E = 69$ GPa, $E_t = 690$ MPa, and $\epsilon_y = 0.00423$, and these material properties are held constant for all subsequent calculations involving the honeycomb model. This bilinear constitutive relationship matches the experimental results reported by Papka and Kyriakides (1994), which correspond to measurements obtained from thin strips of aluminum taken from the honeycomb specimens used in their investigation. This stress–strain relationship holds for the case of monotonic loading, however, elastic unloading also is accounted for by including an appropriate kinematic hardening response law. It should be noted at this point that, as opposed to both the geometric and the material property perturbations that were considered for the truss model, only the geometry of the hexagonal lattice is perturbed for the honeycomb model.

The aluminum honeycomb model is subjected to in-plane, compressive stress states corresponding to uniaxial compression in a direction that is parallel to the thicker cell walls. The macroscopic first Piola–Kirchhoff stress tensor, Π , is given by

$$\Pi = \frac{1}{A_1 A_2} \begin{bmatrix} 0 & 0 \\ 0 & A \end{bmatrix}, \quad (61)$$

where A denotes the macroscopic force parameter and A_1 and A_2 are the dimensions of the honeycomb model in the reference configuration. For the loading conditions presently considered, the macroscopic force parameter, A , may reach a maximum value. Consequently, the work-conjugate quantity, denoted by Δ , is prescribed instead. This macroscopic displacement parameter is given by

$$\Delta = (F_{22} - 1)h, \quad (62)$$

where F_{22} is the only relevant component of the macroscopic deformation gradient tensor, and where h is the out-of-plane thickness of the honeycomb model (here, taken to be unity). Thus, by prescribing the work-conjugate quantity, Δ , the particular load path of interest may be followed in a manner that permits analysis of deformations beyond the maximum load. As with the elastic truss model, the aluminum honeycomb model has been used by the author in previous investigations. For a more complete description of this model, including details concerning the numerical calculations implemented in the solution of the equilibrium equations, see Triantafyllidis and Schraad (1998).

Since it is ultimately the macroscopic stress state that is of primary concern in the vast majority of engineering analyses, the results for the aluminum honeycomb model focus on the influence of perturbations in microstructural periodicity on the dimensionless stress parameter, D , and on the corresponding limit, D_0 . As in the case of the truss model, the principal stress–strain solution for the honeycomb material is obtained first for a model with perfectly periodic microstructure and then for various models with small perturbations in periodicity (again, see Section 3.1 for a more detailed discussion of how these microstructural perturbations are introduced into the models). The solutions for both the periodic model and the nearly periodic models are compared and the convergence of the dimensionless stress parameter is examined, as the geometric scale parameter, ε , decreases. The dependence of the corresponding limit on the perturbation amplitude parameter, δ , is also explored. Additional comparisons are made to provide a more thorough understanding of the manner in which these perturbations affect the macroscopic response of the model. And finally, the actual stress–strain behavior for both the periodic and the nearly periodic honeycomb models is investigated and appropriate comparisons are made.

So first, consider the convergence of the dimensionless stress parameter, D , as the geometric scale parameter, ε , decreases (i.e., as the microstructure of the honeycomb model becomes more refined). Similar to the results presented in Fig. 2a and b for the truss model, Fig. 7a and b shows that D converges to a relatively constant value as ε approaches zero.

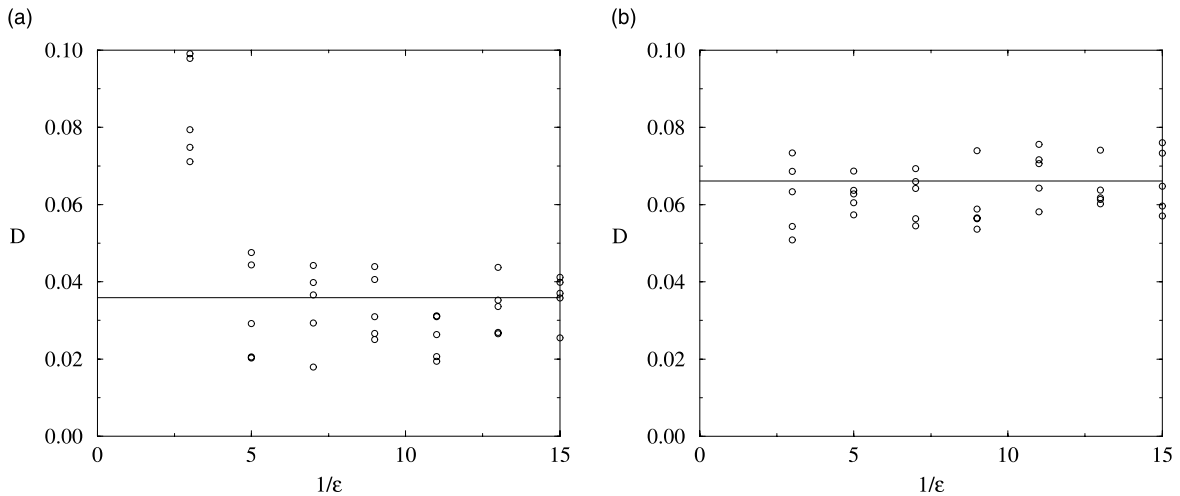


Fig. 7. Convergence of the dimensionless stress parameter as the microstructure of the aluminum honeycomb model is refined. Results are presented for levels of deformation corresponding to: (a) $\Delta = 0.015$; and (b) $\Delta = 0.060$. The solid lines represent limiting values of this parameter as $\epsilon \rightarrow 0$.

In Fig. 7a, the dimensionless stress parameter is determined for various nearly periodic honeycomb models with values of the geometric scale parameter ranging from 0.333 ($N_c = 9$) to 0.067 ($N_c = 225$). To better represent the distribution in material behavior, five different microstructural perturbations are considered for each value of ϵ . Each perturbation corresponds to a different random shape with $\delta = 0.10$. Results are presented for a level of deformation corresponding to $\Delta = 0.015$. At this level of deformation, the behavior of the honeycomb material is still in the linear-elastic regime.

The results are very similar to those presented for the truss model. As expected, the dimensionless stress parameter converges to a relatively constant value as ϵ approaches zero (i.e., as N_c increases). Here, the solid line represents the value of D_0 , which simply is determined for a sufficiently large value of N_c . Again, the variation in D for each value of ϵ indicates that each perturbation shape causes a slightly different macroscopic stress response. The variation in the data for the honeycomb model is greater than that for the truss model, since the geometric perturbations in the honeycomb microstructure can produce significantly different bending stresses in local areas of the model. These differences result in stress responses at the macroscopic scale that reach the onset of plasticity at different points in the macroscopic strain history. As expected, however, the variations in the data for large values of ϵ , which are due to variations in the first-order terms in the expansions of the macroscopic stress tensor Π , decrease as ϵ approaches zero. For small enough values of ϵ the variations in D are due solely to variations in the second-order terms in the expansions of Π .

In Fig. 7b, the same honeycomb models are evaluated, however, the dimensionless stress parameter is evaluated at a level of deformation corresponding to $\Delta = 0.060$. At this level of deformation, the onset of plasticity has been reached and the behavior of the honeycomb material has proceeded well into the plastic regime. Consequently, the material response is no longer hyperelastic, and therefore, it cannot be expected that the dependence of D on the geometric scale parameter will be the same as for the case of purely elastic deformation. At this point in the deformation history, the average value of D remains relatively constant as ϵ decreases. The relatively constant values of D vary only slightly from the value that is determined for the case when ϵ approaches zero (this value is represented by the solid line). Again, these variations are due to differences in the stress response that are produced by the different microstructural geometries of the perturbed honeycomb models. Notice, however, that the values of D at this more progressed stage of

deformation are approximately twice as high as the values determined in the linear-elastic range of deformation. These results do indeed indicate a difference in the scale dependence of the material between the reversible and irreversible regimes of behavior.

Again, as in the case of the truss model, the influence of these perturbations in microstructural periodicity on the macroscopic properties of the honeycomb model is characterized best by examining the dependence of the limit of the dimensionless stress parameter on the perturbation amplitude parameter. In Fig. 8a and b, D_0 is plotted as a function of the perturbation amplitude parameter for aluminum honeycomb models with $\varepsilon = 0.0667$ and for values of δ ranging from 0.00 to 0.10. Here, to expedite the numerical computations, only one perturbation shape is considered for each value of δ . In Fig. 8a, results are presented for a level of deformation corresponding to $\Delta = 0.015$, whereas in Fig. 8b, results are presented for a level of deformation corresponding to $\Delta = 0.060$.

It is quite evident from these results that the limit of the dimensionless stress parameter is influenced by the perturbation amplitude parameter only to second order (i.e., $D_0 \sim O(\delta^2)$) for deformations occurring prior to the onset of plasticity, as suggested by the quadratic dependence of D_0 on δ represented in Fig. 8a. The nature of this dependence changes, however, as the level of deformation increases past the onset of plasticity. In Fig. 8b, this dependence, while nonlinear for very small values of δ , is linear (i.e., $D_0 \sim O(\delta)$) for most of the perturbation amplitude parameter range. As the level of deformation increases and as δ increases, this dependence becomes strictly linear. In any event, for sufficiently refined honeycomb models, the second-order dependence of D_0 on δ is only valid for levels of deformation occurring prior to the onset of plasticity in the parent material.

This same second-order dependence is observed when the individual components of the macroscopic stress tensor are examined. In Fig. 9a and b, the nonzero component of the macroscopic first Piola–Kirchhoff stress tensor, Π_{22} , is plotted as a function of the perturbation amplitude parameter for the same model parameters and levels of deformation as for the results presented in Fig. 8a and b. Again, for deformations occurring prior to the onset of plasticity, the dependence of Π_{22} on δ is second order. This dependence, however, becomes first order as the level of deformation increases past this limiting point. Note, however, that the perturbations in microstructural periodicity in the honeycomb material produce an increase in Π_{22} for deformations in the linear-elastic range, yet a decrease in this stress component is produced as the deformations become more extreme. (Recall that the macroscopic strain energy density

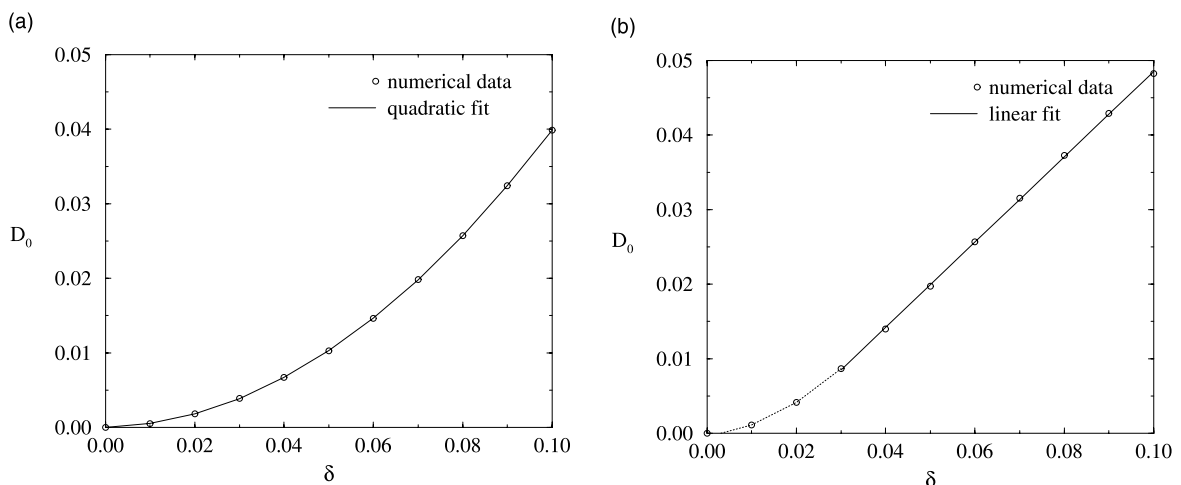


Fig. 8. Limiting values of the dimensionless stress parameter plotted as a function of the perturbation amplitude parameter for levels of deformation corresponding to: (a) $\Delta = 0.015$; and (b) $\Delta = 0.060$. The solid lines represent quadratic and linear fits to these data.

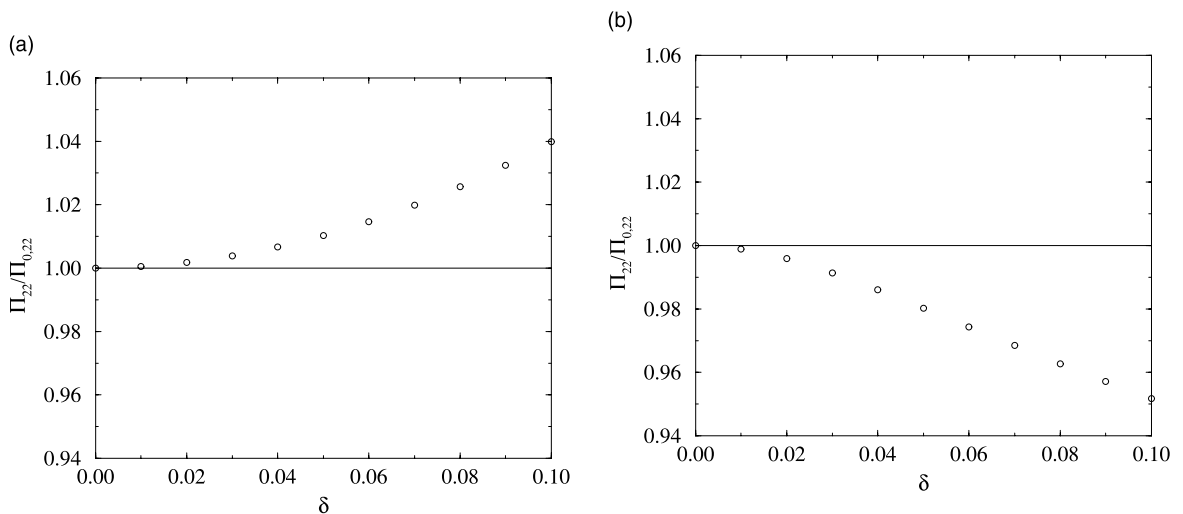


Fig. 9. Normalized values of the macroscopic stress tensor components plotted as functions of the perturbation amplitude parameter for levels of deformation corresponding to: (a) $\Delta = 0.015$; and (b) $\Delta = 0.060$.

experiences a decrease due to perturbations in periodicity, as dictated by Eq. (52).) The slight increase in Π_{22} for small deformations is possible, because the other components of stress, which are identically zero for the periodic case, are nonzero for the model with microstructural perturbations. The results demonstrate the highly nonlinear nature of the honeycomb material response.

Finally, the most illuminating illustration of how perturbations in microstructural periodicity influence the macroscopic properties of the aluminum honeycomb material may be provided by comparing the actual macroscopic stress response of a nearly periodic model with the behavior of the corresponding periodic model. In Fig. 10, the stress response for a honeycomb model with $\epsilon = 0.0667$ ($N_c = 225$) and $\delta = 0.10$ is compared to the behavior obtained for its counterpart with periodic microstructure. Here, the only non-negligible component of the macroscopic stress tensor is plotted. The influence of the microstructural perturbations is indeed very small (i.e., $O(\delta^2)$) for deformations occurring prior to the onset of plasticity, yet becomes substantially more pronounced once this level of deformation is reached. Note that the response is plotted for deformations occurring at the level of the load plateau, which is typically used to determine the practical load-carrying capacity of materials with cellular microstructures. Despite the second-order influence in the linear-elastic range of deformation, the influence of the perturbations along this load plateau becomes first order. For a perturbation amplitude of 10%, one sees roughly a 10% decrease in the load-carrying capacity of the material. The results presented here, demonstrate the importance of considering microstructures that are not perfectly periodic when analyzing structures and materials to determine their failure loads.

5. Concluding remarks

The results of many engineering analyses involving structured media are based on simplifying assumptions concerning the periodicity of the underlying microstructures. For example, homogenization techniques that are used to estimate the macroscopic properties of composite materials, and many structural theories that have been developed to predict the macroscopic response of structural components and

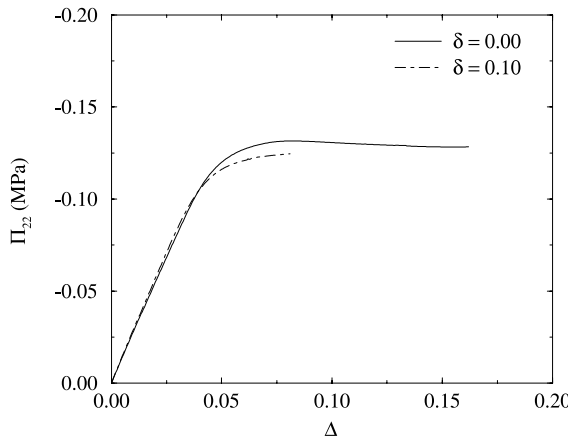


Fig. 10. Macroscopic stress response for aluminum honeycomb models with both periodic and nearly periodic microstructures subjected to uniaxial compression.

cellular materials, assume that the relevant underlying microstructures are perfectly periodic. The structural components and solid materials that are used in actual engineering applications, however, necessarily include microstructural irregularities and defects that result from imperfect manufacturing processes, impurities in materials, and various other types of microscopic and macroscopic damage. From a micromechanics point of view, natural questions arise regarding the influence of these microstructural imperfections on the predicted macroscopic behavior of these structures and materials.

The investigation presented here centers attention on discrete media with periodic and nearly periodic microstructures. For structural trusses, structural frames, and cellular materials, the mechanical response at the macroscopic scale is, in general, easy to define, and the corresponding behavior at the microstructural scale can be characterized in terms of the parameters that govern the stress-strain response of simple, one-dimensional, structural elements. Of particular interest to the present work are structures and solids comprised of materials for which a strain energy density exists – namely, hyperelastic materials. For hyperelastic materials, the macroscopic stresses and the macroscopic incremental moduli can be derived from the macroscopic strain energy density. Analysis, therefore, is focused on the effect of perturbations in microstructural periodicity on the macroscopic strain energy density. More specifically, the macroscopic strain energy density is expanded asymptotically about the periodic solution, and the influence of microstructural perturbations on each term in the expansion is examined.

Following this general analytical approach, two main conclusions are reached. First, the first-order term in the expansion of the macroscopic strain energy density is identically equal to zero. And second, for a given level of deformation, the macroscopic strain energy densities for media with nearly periodic microstructures are necessarily less than the strain energy densities for the corresponding periodic structures and materials. These analytical results hold for discrete structured media exhibiting hyperelastic behavior, provided that the microstructural length scales are small relative to the overall structural or specimen dimensions, and that the parameters that characterize the shapes of the microstructural imperfections satisfy certain criteria (e.g., statistically random imperfections).

The results of several numerical examples are used to highlight the main points of the analytical developments. A nonlinear-elastic truss structure and an elasto-plastic (aluminum) honeycomb material are chosen as two particular models for study. The macroscopic response for each of these structured media is obtained first for the case when the underlying microstructures are modeled as perfectly periodic. For the

truss model, this idealized behavior can be obtained analytically, however, for the honeycomb model, finite-element analysis is used to determine the macroscopic response. The idealized behavior is compared then to the response obtained numerically for the same models after small perturbations in geometry and material properties are introduced into the models at the microstructural scale. The results show that, indeed, the macroscopic properties for the models with nearly periodic microstructures and the macroscopic properties of the corresponding periodic models differ by $O(\delta^2)$, where δ is the perturbation amplitude parameter. The results also show that the energy-carrying capacities of these models are decreased when perturbations in periodicity are introduced into the initially periodic microstructures. These numerical results hold when the microstructures of the models are sufficiently refined and for deformations that occur prior to the onset of failure (e.g., a limit load or the onset of plastic deformation). Results for the aluminum honeycomb model show further that the influence of microstructural perturbations on the macroscopic response becomes first order once the level of deformation reaches the onset of plasticity and leaves the hyperelastic regime of behavior.

The implications of these results can be summarized quite briefly. For structured media comprised of hyperelastic materials, with sufficiently refined, nearly periodic microstructures (i.e., microstructures with small perturbations in periodicity), analysis techniques that are based on assumptions of strict periodicity will not involve significant inaccuracies in macroscopic property predictions, provided that the deformations remain in the hyperelastic regime of behavior. Significant inaccuracies in material property predictions may develop, however, for media with highly irregular or random microstructures, for microstructures with characteristic length scales that are not small compared to the overall structural dimensions, for microstructures with systematic (i.e., nonrandom) imperfections in periodicity, or for media that are subjected to deformations approaching the onset of failure.

Future research will focus on a generalization of the current work to continuous media with nearly periodic microstructures (e.g., composite materials). Some attention also will be given to materials that cannot be characterized as hyperelastic, as well as to materials characterized with rate-dependent constitutive laws. It is hoped that the lessons learned through these investigations will lead to the development of improved continuum theories for microstructured materials – theories that ultimately will use information at the microstructural scale to provide better methods for estimating the macroscopic properties of both discrete and continuous structured media.

Acknowledgements

This work is supported by the US Department of Energy, under contract W-7405-ENG-36. The concepts contained in this work represent a generalization and extension of ideas that were originally formulated, in part, by the author as a graduate student in the Department of Aerospace Engineering at the University of Michigan. As such, the author would like to acknowledge the guidance and counsel offered to him by his former thesis advisor, Professor Nicolas Triantafyllidis. Special thanks are extended as well to Dr. Scott Bardenhagen of the University of Utah for his constructive comments and helpful suggestions.

References

- Antman, S., 1968. General solutions for plane extensible elasticae having nonlinear stress-strain laws. *Quarterly of Applied Mathematics* 26 (1), 35–47.
- Bensoussan, A., Lions, J.L., Papanicolaou, G., 1978. *Asymptotic Analysis for Periodic Structures*. North-Holland, Amsterdam.
- Budiansky, B., 1965. On the elastic moduli of some heterogeneous materials. *Journal of the Mechanics and Physics of Solids* 13 (4), 223–227.

Castaneda, P.P., 1996. Exact 2nd-order estimates for the effective mechanical-properties of nonlinear composite-materials. *Journal of the Mechanics and Physics of Solids* 44 (6), 827–862.

Castaneda, P.P., Willis, J.R., 1995. The effect of spatial-distribution on the effective behavior of composite-materials and cracked media. *Journal of the Mechanics and Physics of Solids* 43 (12), 1919–1951.

Fung, Y.C., 1965. Foundations of Solid Mechanics. Prentice-Hall, Englewood Cliffs, NJ.

Green, A.E., Zerna, W., 1968. Theoretical Elasticity. Oxford University Press, Oxford.

Hashin, Z., Shtrikman, S., 1962a. On some variational principles in anisotropic and nonhomogeneous elasticity. *Journal of the Mechanics and Physics of Solids* 10 (4), 335–342.

Hashin, Z., Shtrikman, S., 1962b. A variational approach to the theory of the elastic behaviour of polycrystals. *Journal of the Mechanics and Physics of Solids* 10 (4), 343–352.

Hashin, Z., 1964. Theory of mechanical behaviour of heterogeneous media. *Applied Mechanics Reviews* 17 (1), 1–9.

Hill, R., 1952. The elastic behaviour of a crystalline aggregate. *Proceedings of the Physical Society of London, Section A* 65 (5), 349–354.

Hill, R., 1963. Elastic properties of reinforced solids: some theoretical principles. *Journal of the Mechanics and Physics of Solids* 11 (5), 357–372.

Hill, R., 1965. A self-consistent mechanics of composite materials. *Journal of the Mechanics and Physics of Solids* 13 (4), 213–222.

Love, A.E.H., 1944. A Treatise on the Mathematical Theory of Elasticity. Cambridge University Press, Cambridge.

Mendenhall, W., Wackerly, D.D., Scheaffer, R.L., 1990. Mathematical Statistics with Applications. PWS-KENT, Boston (Chapter 4).

Nemat-Nasser, S., Hori, M., 1993. Micromechanics: overall properties of heterogeneous materials. Elsevier, Amsterdam.

Noll, W., 1955. On the continuity of the solid and fluid states. *Journal of Rational Mechanics and Analysis* 4, 3–81.

Papka, S.D., Kyriakides, S., 1994. In-plane compressive response and crushing of honeycomb. *Journal of the Mechanics and Physics of Solids* 42 (10), 1499–1532.

Reuss, A., 1929. Berechnung der Fliessgrenze von Mischkristallen auf Grund der Plastizitätsbedingung für Einkristalle. *Zeitschrift für Angewandte der Mathematik und Mechanik* 9 (1), 49–58.

Sanchez-Palencia, E., 1974. Comportements local et macroscopique d'un type de milieux-physiques hétérogènes. *International Journal of Engineering Science* 12 (4), 331–351.

Schraad, M.W., Triantafyllidis, N., 1997a. Scale effects in media with periodic and nearly periodic microstructures – Part I. Macroscopic properties. *Journal of Applied Mechanics* 64 (4), 751–762.

Schraad, M.W., Triantafyllidis, N., 1997b. Scale effects in media with periodic and nearly periodic microstructures – Part II. Failure mechanisms. *Journal of Applied Mechanics* 64 (4), 763–771.

Talbot, D.R.S., Willis, J.R., 1985. Variational principles for inhomogeneous nonlinear media. *IMA Journal of Applied Mathematics* 35 (1), 39–54.

Talbot, D.R.S., Willis, J.R., 1997. Bounds of 3rd-order for the overall response of nonlinear composites. *Journal of the Mechanics and Physics of Solids* 45 (1), 87–111.

Triantafyllidis, N., Schraad, M.W., 1998. Onset of failure in aluminum honeycombs under general in-plane loading. *Journal of the Mechanics and Physics of Solids* 46 (6), 1089–1124.

Voigt, W., 1889. Ueber die Beziehung zwischen den beiden Elasticitätsconstanten isotroper Körper. *Annalen der Physik und Chemie* 38 (12), 573–587.

Voigt, W., 1928. Lehrbuch der Kristallphysik. Teubner, Leipzig.

Willis, J.R., 1977. Bounds and self-consistent estimates for the overall properties of anisotropic composites. *Journal of the Mechanics and Physics of Solids* 25 (3), 185–202.